University of La Laguna

Department of Physics

Global optimization in complex molecular systems

Author:
Raquel González Armas

Supervisor:
Dr Javier Hernández Rojas

Final degree project

Degree of Physics

July 9, 2019

Acknowledgements

I would like to express my sincere gratitude to my supervisor Dr Javier Hernández Rojas, for guiding me during all the project, for his patience and for his clarifying explanations. Also, to all the professors of the degree, since they have provided me with a solid scientific education and inspired me in many different ways.

And last but not least, to my classmates, for sharing their different points of views, helping me in many occasions, teaching me useful tools and, of course, for making the degree much more entertaining.

Abstract

The global optimization is a field of growing interest and developing due to the wide variety of applications that presents. One of them is treated in this project: the search of global energy minimum structures for clusters interacting with a Lennard-Jones or Improved Lennard-Jones potential. Three known methods for treating this problem are explained: genetic algorithm, simulated annealing and basin-hopping. The last one has been implemented for clusters containing up to 50 atoms. By means of the results, the main features of the structures and energies of this type of clusters are analysed.

La optimización global es un campo de creciente interés y desarrollo debido a la amplia variedad de aplicaciones que presenta. Una de ellas es tratada en este proyecto: la búsqueda de estructuras de mínima energía para agregados de átomos interaccionando mediante el potencial de Lennard-Jones o el potencial de Lennard-Jones mejorado. Tres conocidos métodos para tratar este problema son explicados: el algoritmo genético, el algoritmo de enfriamiento simulado y el algoritmo de salto de pozos o cuencas. Este último ha sido programado para agregados que contienen hasta 50 átomos. A partir de los resultados obtenidos, las principales características de las energías y las estructuras de este tipo de agregados son analizadas.

Contents

List of Figures

List of Tables

Chapter 1

Introduction

Finding the global optimum solution for a problem is of great interest in many fields as economics and science. Particular cases are the design of microprocessor circuitry and the travelling salesman problem [1]. However, we are going to focus on the relevance that the global optimization methods have in cluster science.

The potential energy surface (PES) is a function of all the interactions between atoms or molecules, and although the system was very simple, the PES might have a large number of local minima.

Following D. J. Wales, "The structure and dynamics of atomic and molecular clusters, the folding of proteins, and the complicated phenomenology of glasses are all manifestations of the underlying potential energy surface (PES)"[2]. Moreover, in many situations the structure that adopts the system is related to the global minimum of the PES or the free energy surface [3].

The dynamic properties of a system depends upon how the local minima are connected, while the thermodynamic behaviour depends on the relative potential energy of the local minima and the volumes of the conformation space associated with them [2].

The rare gas clusters were the first to be studied experimentally. They are quite well modelled by the Lennard-Jones (LJ) potential (from Ne to Xe) which is easy to implement [2]. However, it is a hard problem to optimize because the number of local minima increases exponentially with the number of atoms according to empirical evidence [3]. These clusters, up to 100 atoms, are based on the icosahedral packing. There are a few exceptions as LJ_{38} and LJ_{75-77}. These cases are convenient for testing the heuristic global optimization algorithms because the minimum, corresponding to the icosahedral configuration, acts like a trap and it is far from the global minimum [1]. For this reason, they are excellent to distinguish between an useful or useless method. Recently the Improved Lennard-Jones potential (ILJ) was proposed by F. Pirani et al. [4]. It is more accurate than the LJ, specially for long and short ranges. Moreover, it is able to describe systems which contain ions. Therefore, it may allow the comprehension of many other unknown systems [4].

There have been several global optimization methods that have attempted to find the global minimum of the LJ clusters. Among them, it is the simulated annealing [3]. This method may be the first generally applicable global optimization algorithm, and many variations of itself have been explored [2]. However, this method show

many inconveniences when the number of atoms increases and when the PES is more complicated. The chapter 3 provides an insight into this method.

On the other hand, the genetic algorithm is a powerful optimization technique. It have been proved to be very efficient for the structural minimisation of clusters, but also for the prediction of protein secondary and tertiary structure and the simulation of protein folding [5]. This method is also explained in the chapter 3.

The last method that is mentioned in the project is the basin-hopping [6]. The approach have achieved promising results as finding in an unbiased search the global energy minimum for LJ_{75}. The algorithm is discussed in the chapter 3 and programmed in the chapter 4 for LJ and ILJ potentials.

Eventually, I would like to emphasise that the interest of the global optimization methods in the study of clusters is not just about finding the global minimum or local minima close to the global minimum, although, that is obviously what a good optimization method is supposed to do. Further on, they enable us to realise if a potential is physically reasonable or not for a certain type of cluster [5].

1.1 Objectives

The motivation of this project is to present an overview of the global optimization methods currently applied to find the native geometry corresponding to LJ and ILJ clusters and to program one of them: the basin-hopping method.

First of all, the chapter 2 provides a background information about the potential energy surface, a brief overview of the inter-atomic potential, and an explanation of the both mentioned above.

In chapter 3, we discuss about three common global optimization methods applied to this type of cluster: genetic algorithm, simulated annealing and basin-hopping.

In the chapter 4 the basin-hopping method is explained clearly through the explanation of the way we implemented the simulation. In this same chapter, the results of the global energies minima are presented.

Chapter 5 covers the stability of cluster through the interpretation of the second-order energy difference obtained. In addition, some of the most special geometries found are represented and explained, together with information about our difficulty or facility of finding the global minimum.

The last chapter 6 contains an assessment of the project, which includes possible improvements of the work we have done and different ways of continuing the project.

1.2 Summary in Spanish

Encontrar la solución óptima para un problema complejo es de gran importancia para diferentes campos de la ciencia y la economía. Nosotros nos centraremos en la relevancia que tienen los métodos de optimización global en la ciencia de agregados. Más concretamente, en los agregados de átomos que interaccionan según el potencial

de Lennard-Jones y el Lennard-Jones mejorado.

En el capítulo 2 se explicará el origen cuántico de la superficie de energía potencial y los dos tipos esenciales de potenciales interatómicos que hay: potenciales a pares y de muchos cuerpos. Por otro lado, se hablará del LJ e ILJ, destacando las ventajas del ILJ con respecto a su antecesor.

Los métodos de optimización global más destacados para tratar este tipo de agregados son introducidos en el capítulo 3. Se explica el algoritmo genético y el algoritmo de enfriamiento simulado de forma bibliográfica, tras una introducción del problema matemático que supone la optimización global. Al final del capítulo, se habla brevemente del método de salto de pozos (BH).

El método de salto de pozos es tratado con más profundidad en el capítulo 4, mediante la explicación de la programación realizada. En este capítulo se muestran los resultados de las mínimas energías conseguidas.

En el capítulo 5, se habla de las simetrías que suelen presentar este tipo de agregados. Resaltando algunas de ellas como el icosaedro de 13 átomos o el octaedro truncado de 38 átomos, debido a su especial estabilidad y a la dificultad que supone encontrar la configuración de mínima energía, respectivamente.

En el último capítulo, el capítulo 6, se realiza una valoración del trabajo. En ella se incluyen posibles mejoras que se podrían realizar al trabajo y diferentes formas para continuar el proyecto.

Chapter 2

Lennard-Jones and Improved Lennard-Jones potentials

Choosing a suitable potential energy function is essential in order to determine the ground state of a system as the global minimum configuration of the potential energy surface. In this chapter, we discuss why we can talk about the potential energy surface, through the explanation of a fundamental approximation in molecular physics: the Born-Oppenheimer approximation. After that, an overview of the inter-atomic potentials is given. Then, the venerable Lennard-Jones potential and the Improved Lennard-Jones are explained, together with a reflection of the enhancements the Improved Lennard-Jones brings.

2.1 Born-Oppenheimer approximation

Throughout the introduction we have talked about the potential energy surface or free energy surface. However, how can we evaluate the energy of an atomic system by only taking into account the positions of the nuclei? What about the electrons? The Born-Oppenheimer approximation give us the answer that enable us to consider the very notion of potential energy surface [2].

Suppose a system with n electrons, with mass m_e and positions $\mathbf{x} = \{x_i\}$ and N nuclei, with mass M_t and positions $\mathbf{X} = \{X_t\}$. The corresponding time-independent Schrödinger equation is

$$\left[-\sum_{t=1}^{N} \frac{\hbar^2}{2M_t} \nabla_t^2 - \sum_{i=1}^{n} \frac{\hbar^2}{2m_e} \nabla_i^2 + V(\mathbf{x}, \mathbf{X}) \right] \psi(\mathbf{x}, \mathbf{X}) = E_{total} \psi(\mathbf{x}, \mathbf{X}) \quad , \tag{2.1}$$

being the potential energy

$$V(\mathbf{x}, \mathbf{X}) = \frac{e^2}{4\pi\epsilon_0} \left[-\sum_{i,t}^{n,N} \frac{Z_t}{r_{it}} + \sum_{i<j} \frac{1}{r_{ij}} + \sum_{t<s} \frac{Z_t Z_s}{r_{ts}} \right] \quad , \tag{2.2}$$

Z_t is the atomic number of the nucleus labelled t, $\hbar$ is the reduced Planck constant, e is the charge of the electron and ϵ_0 is the absolute dielectric permittivity

of vacuum. The distance between the electron labelled i and the nucleus labelled t is r_{it}. Similarly, the separation between the electrons labelled i and j is r_{ij} and between the nuclei t and s is r_{ts}. The terms of the potential are the electron-nucleus, the electron-electron and the nucleus-nucleus Coulomb interaction.

The distance term r_{it} (electron-nucleus interaction) prevent our Hamiltonian from being separable. Nevertheless, due to the huge difference between the mass of the nuclei and the electron ($m_p \approx 1836 m_e$, being m_p the mass of the proton), Born and Oppenheimer reasoned that the electron density should adjust almost instantaneously to changes in the position of the nuclei [2]. The approximation of the wave-function is

$$\psi(\mathbf{x}, \mathbf{X}) = \psi_e(\mathbf{x}; \mathbf{X})\psi_n(\mathbf{X}) \quad , \tag{2.3}$$

where ψ_e represent the solution of the electron Hamiltonian. The electronic part satisfies the equation

$$[\hat{H} - \hat{T}_n]\psi_e(\mathbf{x}; \mathbf{X}) = V_e(\mathbf{X})\psi_e(\mathbf{x}; \mathbf{X}) \quad , \tag{2.4}$$

being $\hat{H}$ the total Hamiltonian operator, which is the term in square brackets of the equation 2.1, and $\hat{T}_n$ the nuclear kinetic energy operator which corresponds with the first term of the expression 2.1. The electronic wave-function depends upon the positions of the electrons and upon the nuclei positions parametrically. Nuclear positions appeared as fixed points because the equation 2.4 is solved for each nuclear configuration.

The potential energy surface defines the variation of the electronic energy, $V_e(\mathbf{X})$ with the nuclear geometry. We form the PES with the ground electronic configuration that it is the most likely configuration at low temperatures. Moreover, the first excited may not be a bound state.

Eventually, if we want to find the total wave-function, we have to solve the nuclear part of Schrödinger equation.

$$[\hat{T}_n(\mathbf{X}) + V_e(\mathbf{X})]\psi_n(\mathbf{X}) = E_{total}\psi_n(\mathbf{X}) \tag{2.5}$$

2.2 Inter-atomic potentials

The energy of a system of N atoms interacting according to a certain potential can be expanded as the following

$$U(\vec{r_1}, \vec{r_2}...\vec{r_N}) = \sum_{i}^{N} U_1(\vec{r_i}) + \sum_{i}^{N}\sum_{j<i}^{N} U_2(\vec{r_i}, \vec{r_j}) + \sum_{i}^{N}\sum_{j<i}^{N}\sum_{k<j} U_3(\vec{r_i}, \vec{r_j}, \vec{r_k}) + ... \tag{2.6}$$

The first term, U_1, is due to an external field or to boundary conditions. U_2 takes into account the interaction between each pair of particles that are part of the system, the presence of the other atoms does not affect. It is necessary to impose the condition $j < i$ in order to count the pairs only once. In the term U_3, we consider the influence of a third atom presence.

Based on this expansion the inter-atomic potentials can be classified in two groups: pair potentials and many-body potentials. The first group only takes into account U_2 (when we set U_1 to zero considering that there isn't an external field), whilst the second group of potential considers higher potential orders. The potentials used in this project are pair potentials.

2.3 Description of the Lennard-Jones potential

The Lennard-Jones potential describes the potential energy of interaction of a two non-bonding atoms or molecules based on the distance between them. It was suggested by Mie in 1903 and later, it was proposed by Sir John Edward Lennard-Jones in 1924. Although it is not the most accurate model for the interaction between rare gas atoms, it is considerably widespread because of its computational expediency. In addition, it is remarkable that many of the global minimum structures have been observed experimentally for clusters of atoms covering a wide range of the periodic table [2]

The Lennard-Jones potential consists in two contributions: a steep repulsive term, and a smoother attractive term. The repulsive term is the result of the repulsion between the electrons clouds of the atoms or molecules when they are close enough. By contrast, the dipole-induced dipole-induced interaction between particles is the cause of the attractive contribution. The functional form of this potential is the following:

$$V_{LJ}(r) = 4\epsilon \left[\left(\frac{\sigma}{r}\right)^{12} - \left(\frac{\sigma}{r}\right)^{6} \right] \quad , \tag{2.7}$$

where ϵ is the depth of the potential well, σ is the finite distance at which the inter-particle potential is zero and r is the distance between particles.

The second term which appeared in the expression (2.7) is the attractive one. Due to this term the atoms tend to come closer each other until the first term of the equation, the repulsive one, has a significant contribution.

In order to simplify the units, we are going to set $\epsilon = 1$ and $\sigma = 1$ hereinafter.

In the two particle system it is trivial to find the overall minimum which is assumed at a distance $2^{1/6}$ with energy -1. In the figure 2.1, it's shown the energy landscape for the two particle system for both LJ and ILJ potentials. We can see that when the distance between particles tends to zero the energy diverges. On the other hand, when the distance becomes very large, the energy contribution decreases until being virtually null.

2.4 Improved Lennard-Jones potential

The Lennard-Jones potential is widely used in Molecular Dynamics and Monte Carlo methods. It is well known that this model is highly accurate in the equilibrium range. However, it overestimates the strength of the long range attraction and short range repulsion. It is remarkable that the Improved Lennard-Jones only involves

a new parameter with respect to the Lennard-Jones potential. That's one of the reasons why it is called "Improved Lennard-Jones" [4].

The ILJ potential has the analytical form

$$V_{ILJ}(r) = \epsilon \left(\frac{m}{n(r) - m} \left(\frac{r_m}{r} \right)^{n(r)} - \frac{n(r)}{n(r) - m} \left(\frac{r_m}{r} \right)^{m} \right) \quad , \tag{2.8}$$

where ϵ and r_m represent respectively the depth of the potential well and its location. $n(r)$ is a function that depends on r

$$n(r) = \beta + 4 \left(\frac{r}{r_m} \right)^2 \quad , \tag{2.9}$$

β is a parameter related to the hardness of the two interacting particles. In this project, it is going to be assumed constant, fixed to 9 [4].

A direct advantage of this potential with respect to LJ is its capacity of describing systems that are composed of ions. The factor m assumes the value $m = 6$ for neutral-neutral system, $m = 4$ for ion-neutral systems and $m = 1$ for ion-ion systems.

In order to place the overall minimum at the same distance for both potentials in the two-particle system, we have to impose $r_m = 2^{1/6}$. That's what we have done hereinafter.

In the figure 2.2, we can observe that the behaviour around the equilibrium distance is qualitatively the same for both potentials. In the figure 2.2, we can see that in the nearest region to the equilibrium distance, the Lennard-Jones potential has lower energy than the ILJ. Nevertheless, in figure 2.3 it is shown that the LJ behaviour at shorter distances is steeper than the one estimated through the ILJ. The ILJ behaviour describes better the experimental measures.

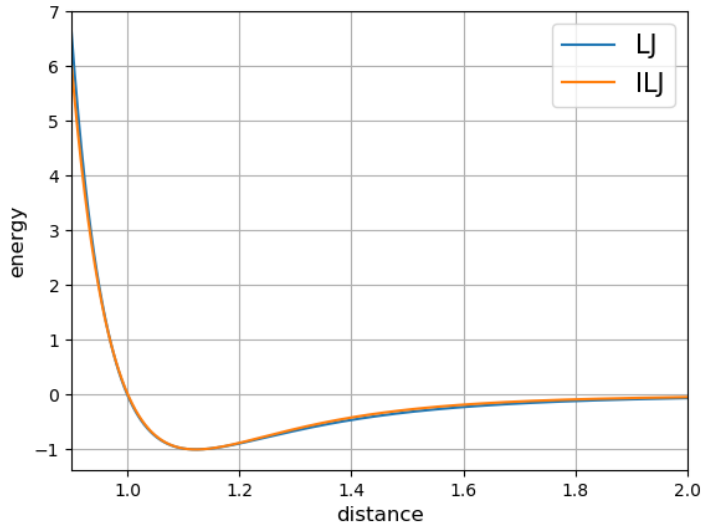

Figure 2.1: Representation of the LJ and ILJ potentials in the two-particle system. Set units ($\epsilon = 1$, $\sigma = 1$, $r_m = 2^{1/6}$)

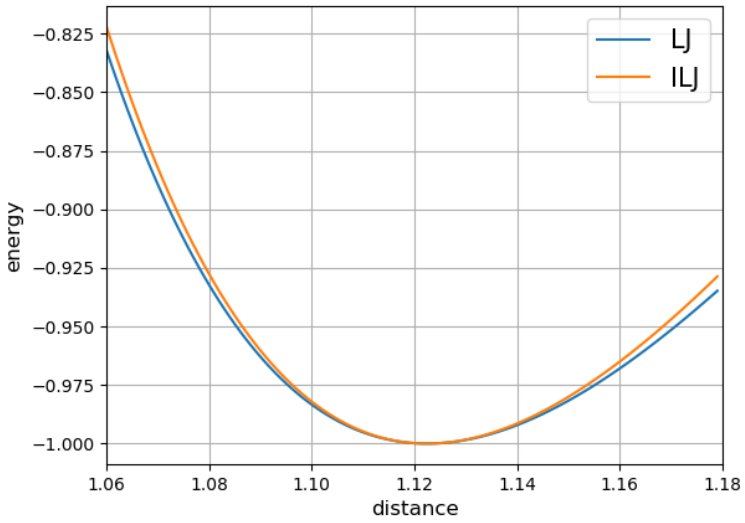

Figure 2.2: Comparison of the nearest equilibrium range behaviour. Set units ($\epsilon = 1$, $\sigma = 1$, $r_m = 2^{1/6}$)

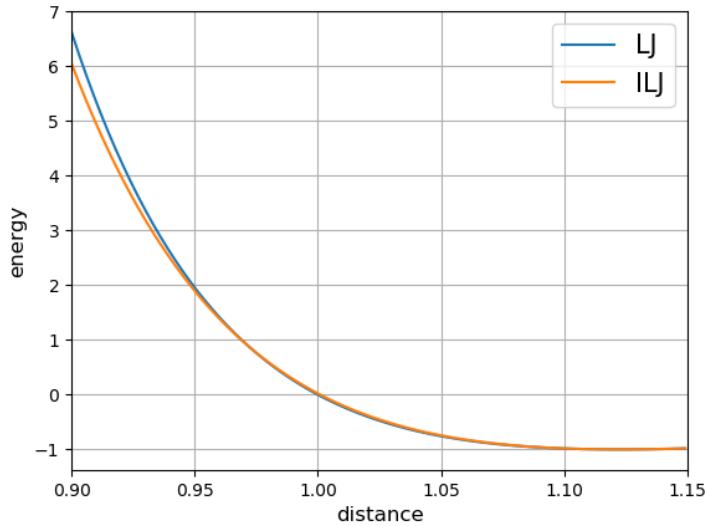

Figure 2.3: Comparison of the short distance behaviour. Set units ($\epsilon = 1$, $\sigma = 1$, $r_m = 2^{1/6}$)

2.5 Summary in Spanish

Elegir un potencial de interacción entre átomos es esencial a la hora de encontrar la estructura molecular de mínima energía global. La definición de superficie de energía potencial (PES) surge de la aproximación de Born-Oppenheimer. En ella se supone que al ser los electrones mucho más ligeros que los núcleos, es posible desacoplar los movimientos electrónico y nuclear.

Los potenciales pueden diferenciarse en dos tipos: a pares y de muchos cuerpos. Los primeros de ellos, solo tienen en cuenta las interacciones de pares de partículas y dependen únicamente de la distancia entre ellas. El potencial de Lennard-Jones es un potencial a pares de uso bastante frecuente, describe considerablemente bien el comportamiento de los gases nobles (desde el Ne hasta el Xe) y es muy sencillo de evaluar en sistemas de átomos neutros. Una mejora reciente de este potencial, el Lennard-Jones mejorado, permite además describir sistemas que contienen iones. Su comportamiento en la región de equilibrio es prácticamente el mismo que el LJ, sin embargo, a mayores y menores distancias su comportamiento se asemeja más a los datos experimentales.

Chapter 3

Global optimization methods

In this chapter, some of the most widespread heuristic methods for the global optimization problem will be introduced. A general introduction of the global and local optimization problem is followed by a description of the genetic algorithm, simulated annealing technique and a summery of the basin-hopping method. The basin-hopping method is explained more extensively together with the simulations made in the next chapter.

3.1 Introduction

Global optimization is a branch of applied mathematics and numerical analysis whose goal is to find the optimal value of a function from all possible solutions. This concept differs from the local optimization. A local optimum is an optimal solution within a neighbouring set of solutions. Let's illustrate it with the mathematical definitions.

Let f be a function of x defined on the interval $x \in \Omega$.

$f(x*)$ is a local minimum if there exist a $\delta > 0$ such $f(x*) \leq f(x)$ for all $x \in \{x \in \Omega : |x - x*| \leq \delta\}$

By contrast, a global minimum is the smallest function value over all feasible points: $f(x*) \leq f(x)$ for all $x \in \Omega$.

Same definitions are valid for the global and local maximum by only changing $f(x*) \geq f(x)$

There are multiple methods for solving local optimization problems: line search methods, steepest descent, Newton's method, Quasi-Newton methods, conjugate gradients methods, etc [7]. All of them depend on the initial guess. In the global optimization methods, we normally need some local optimization routine.

As it has been said before, finding the optimal solution for a problem is of great importance in many science and economic fields, from the travelling salesman problem to the design of microprocessor circuitry [1]. The first simple approach we can think for searching an optimum value may be choosing a random point of the function and using a local optimization method. Through the repetition of this process, it is likely we find the global optimum. The problem arises when

the function has a lot of minima or maxima since the method would need a huge amount of computational time to obtain the solution [3]. This is the case of cluster optimization problems. For instance, it is estimated at least 10^{10} minima in the PES of the cluster LJ_{55} [1]. A curious thought experiment related is the Levinthal's paradox. It says, in essence, that finding the native structure for a folded protein by a random search takes an enormous amount of time, while proteins can fold in a matter of seconds or less [8]. For this reason, researchers has created heuristic algorithms that emulate some natural processes.

3.2 Genetic algorithm

The genetic algorithm is an evolutionary algorithm. It was proposed by John Holland in 1960, although, the use for optimizing cluster geometries was pioneered in the 1990's by Hartke [5]. It is based on the theory of natural evolution. As it happens in nature, the algorithm represents the processes of mating or crossover, mutation and natural selection by using three operators.

The process begins with a set of individuals which is called initial population. The initial population is usually chosen randomly. However, in some cases it may be interesting to have a prior knowledge, avoiding biasing the search too much [5]. The individuals are also known as chromosomes or strings of variables and they are featured by its genes and alleles. In this context, the genes are the variables to be optimized, whilst the alleles are the values of the variables. The figure 3.1 may clarify the previous exposed concepts.

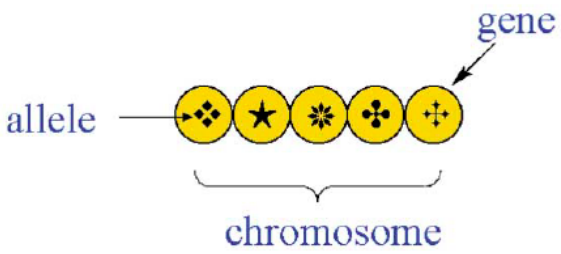

Figure 3.1: Representation of a chromosome or individual with its genes and alleles. Image extracted from reference [5].

For this algorithm to succeed in finding the global optimum, it is essential to measure the quality of the trial function which is represented by the chromosome. The fitness provides that measure. Fitness determines the likelihood of being chosen for the crossover process and surviving into the next generation.

Generating "offspring" is creating a new individual throughout the combination of the genetic information of two individuals, commonly named as parents (crossover). In order to select the two parents, the two more usual methods are the "roulette wheel" and "tournament". In the first one, you choose an individual randomly, if its fitness value is greatest than a random number uniformly distributed between 0 and 1, that individual is selected. If it is lower, you repeat it with another individual until one satisfies the requirement. In the "tournament" method, a set of individuals is chosen randomly. The two individuals that had the highest fitness are selected.

Once the "parents" have been selected, there exist several forms of combining the genes in the "offspring". They differ from each other depending on which part of the sequence they take from the "parents", if the genes maintain the order they had or if the genes reorder randomly in the "children". The figure 3.2 illustrates two common forms of crossover that maintain the order.

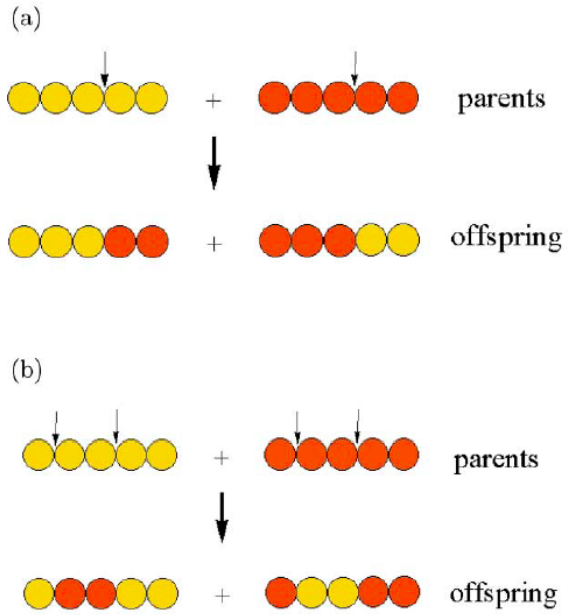

Figure 3.2: Two different forms of combining the genes. (a) One-point crossover and (b) two-point crossover. Image extracted from reference [5].

The crossover process mixes the genes from one generation to the next, but it doesn't introduce new genes. By contrast, mutation operator helps to increase population diversity by making a random change to some genes in an individual. Introducing new genes is important in order to prevent population from converging into a non-optimal solution [5].

The genetic algorithm creates generation after generation until it converges into a solution. There are variety of convergence criteria. One of them is to fix a number of iterations and the algorithm will simply stop running in the last generation. Another is to stop when the best fitness value of the generation is changing by a small fixed amount.

3.3 Simulated annealing

The term annealing is widely used in metallurgy. Annealing is a heat treatment that involves heating a material above its crystallization temperature and maintaining a suitable temperature in order to ensure the thermal equilibrium between particles, followed by a controlled cooling. It is useful for increasing the size of the crystals and for reducing the imperfections. This technique has inspired the simulated annealing algorithm.

This method needs a random perturbation or move that creates a new solution from another previous and a criteria for deciding if the new solution is accepted or not. It was quickly applied to cluster problems by means of the Monte Carlo

method. In particular, it is used the Metropolis algorithm in which moves are accepted according to a Boltzmann probability, $e^{-\Delta E/k_B T}$, where $\Delta E = E_{i+1} - E_i$ is the energy difference between two states, k_B is the Boltzmann constant and T is the temperature [3].

The basic iteration consists in comparing the current state with another in its neighborhood, and deciding between moving to the new solution or staying in the old one. In the case of clusters, the new set of positions are generated through the application of the next random perturbation to each coordinate.

$$x_{i+1} = x_i + 2s(\delta - 0.5) \quad , \tag{3.1}$$

where δ is a random number uniformly distributed between 0 and 1. The acceptation of the new solution is affected by the parameters s and T. A greater s, allows the method to pick randomly the new solution from a wider interval. The temperature affects directly to the Boltzmann probability.

If $E_{i+1} < E_i$, the new solution is accepted immediately. However, if $E_{i+1} > E_i$, the new solution may be accepted if it satisfies

$$e^{-\Delta E/k_B T} > \gamma \quad , \tag{3.2}$$

being γ a random number uniformly distributed between 0 and 1.

Early in the search, the temperature is higher and simulated annealing explores freely the configuration space. For each temperature a number of iterations are performed. The temperature decreases logarithmically as $T \to \chi T$ with $\chi < 1$ [3]. When the search progresses and the temperature is lower, the simulated annealing become greedy and accept much less sets of solutions.

A disadvantage of the method is that it is easy to get trapped in a local minimum and don't explore all the configuration space. Such effect can be reduced by decreasing slower the temperature.

The flowchart 3.3 may clarify the steps taken in the simulated annealing.

3.4 Basin-hopping

The algorithm in its current form was described by David J. Wales and Jonathan P. K. Doye in 1997. The method consists in a transformation of the potential energy surface which does not change the global minimum. With this technique the energy at each point in the configuration space is assigned to a local minimum. In the figure 3.4 the energy transformation is shown for a one dimensional problem [6].

This technique has been proved to locate successfully the lower energy structures up to $N = 110$ for the Lennard-Jones clusters. Moreover, it is remarkable that it has been the first unbiased search method to find the global minimum for LJ_{75} and LJ_{102} clusters, which are based on the Mark's decahedron structure [6].

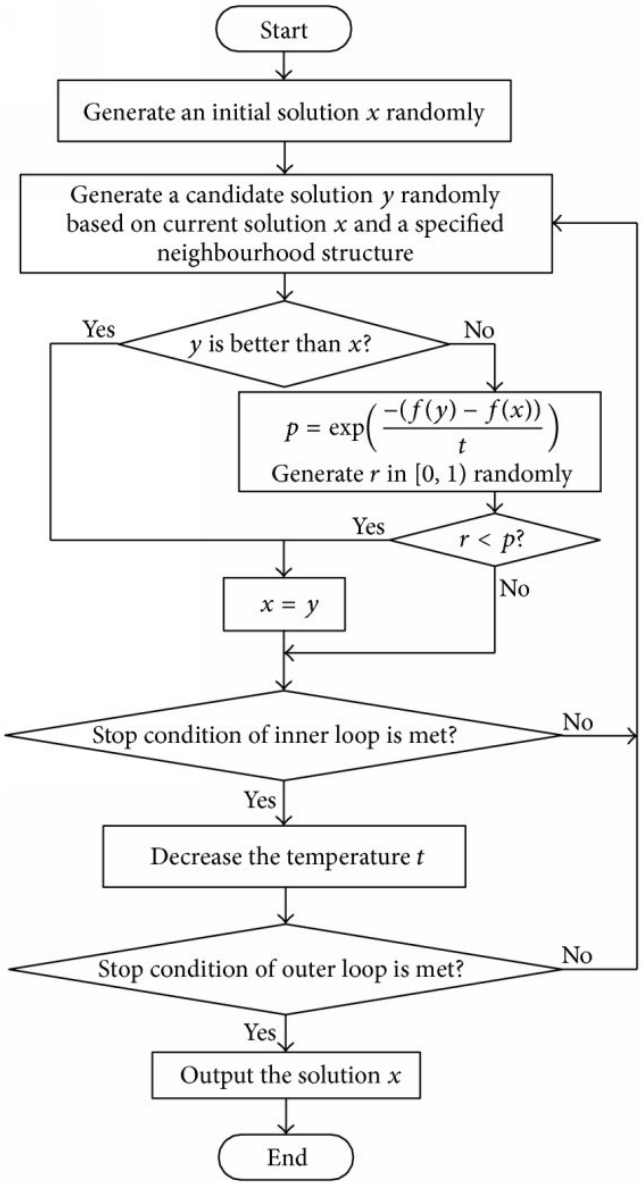

Figure 3.3: Flowchart of the simulated annealing, extracted from reference [9]. Set units ($k_B = 1$).

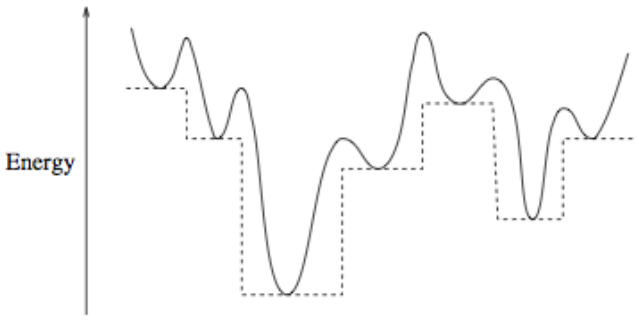

Figure 3.4: Energy transformation for a one dimensional example. Image extracted from reference [6]

3.5 Summary in Spanish

La búsqueda del valor óptimo de una función es de gran importancia en diferentes campos de la ciencia y de la economía. Se trata de un problema matemático de gran dificultad cuando la superficie de energía potencial o la función tienen un gran número de mínimos, y es por ello, por lo que los científicos han diseñado algoritmos heurísticos que permitan reducir el tiempo computacional. Entre estos algoritmos se encuentra el algoritmo genético, el cual se basa en la teoría natural de la evolución, representando con operadores los procesos de selección, mutación y apareamiento. Por otro lado, se tiene el simulated annealing o algoritmo de enfriamiento simulado que se basa en perturbar el estado original para obtener otro nuevo y decidir probabilísticamente si cambiar o no de estado. La temperatura infuye en la probabilidad de aceptación, cuanto mayor es, más explora el espacio de configuración y viceversa. La temperatura disminuye a medida que avanza el proceso. Este algoritmo tiene la desventaja de quedarse atrapado en mínimos locales y no ser capaz de salir de ellos una vez la temperatura ha disminuido. Esta desventaja no la tiene el algoritmo de salto de pozos (BH). Consiste en una transformación de la superficie de energía potencial, que no modifica el mínimo global y suaviza la PES, y es la primera técnica no dirigida que ha conseguido encontrar el mínimo global para LJ_{75} y LJ_{102}

Chapter 4

Simulations

In the project, the global minimum structures of the clusters up to 50 atoms have been obtained for both LJ and ILJ potentials by means of the basin-hopping algorithm. The clusters considered are composed by neutral atoms and we have used, as we mentioned before, the units where $\sigma = 1$, $\epsilon = 1$ and $r_m = 2^{1/6}$ in the equations 2.7 and 2.8. But also, in order to simplify even more, in the units used $k_B = 1$. In this chapter, all the significant steps taken for the implementation of the algorithm and the results obtained for the energies are fully discussed.

4.1 Basin-hopping: the method followed

In first place, an initial state must be supposed. As we want to do an unbiased search, it is going to be set randomly. An easy form and the one that we have used, is to place the N atoms inside a sphere of radius 3.

Once we have the distribution, it is applied a local minimisation

$$V(\vec{X}) = min\{V(\vec{X})\} \tag{4.1}$$

It is important to realise that the equation 4.1 is applied to each new configuration, not to the whole potential energy surface [2].

When the minimization is performed, it is vital that the atoms were still inside the sphere, otherwise the result could be an atom far from the others and a local minimum configuration of the remaining atoms. If the isolated atom was far enough, through the perturbation it wouldn't reach the others. Consequently, the global minimum of the whole cluster couldn't be obtained in that trajectory.

The next step is to perturb the state in order to obtain another new state in the neighbourhood of the original. The process used is the one also explained for the simulated annealing in the previous chapter. Through the equation 3.1, a new state is generated and then, local minimized by means of the application of the expression 4.1.

The states are compared according to a Boltzmann probability as it is applied in the simulating annealing.

This process is repeated until a convergence criteria is acquired. We have just set a number of steps depending on the number of atoms and the difficulty of finding the global minimum. Thanks to the Cambridge Energy Landscape Database [10], we have had the ability of compare our results for the Lennard-Jones clusters. For the Improved Lennard-Jones, we have used a new database [11].

As this method carries a lot of computational time, it is interesting to reduce it as much as we are capable. Apart from changing and simplifying the code in order to make it less time-consuming, we can modify three parameters in order to achieve a better performance. They are the sintetic temperature (T), the step (s) and the local minimization search routine. The first two parameters affect the acceptance rate of solutions, which is the number of solutions accepted divided by the number of iterations performed.

The temperature is usually fixed by running several trajectories for a cluster at different temperatures. The temperature selected will be the one that obtains the global minimum in the lowest number of steps. In the table 4.1 the means of the lowest step, in which the global minimum was achieved, for different temperatures are shown in the case of LJ_{13} cluster. Each mean was calculated with 15 trajectories and the number of iterations was fixed to 500. According to the results, the best temperature in this case is 0.8.

T	0.5	0.6	0.7	0.8	0.9	1.0
Step	17.26	21.33	18.33	15.00	22.00	21.53

Table 4.1: Data for determining the best temperature for LJ_{13}

However, I would like to highlight that this procedure to fix the temperature to its optimal value can only be made by knowing the global minimum beforehand. And as D. J. Wales said in the reference [2]: "finding optimal parameters for a problem that is already solved is probably only worthwhile if those parameters are then close to optimal for other problems of interest". We have fixed the temperature to 0.8, but it may not be the optimum temperature for all the clusters studied. If we are studying clusters containing a few atoms, the global minimum will be probably known and this procedure could be applied. When the size of the clusters increases, we can change the temperature for different trajectories in order to see what minima it detects depending on the temperature and select the one which implies better results.

By the other hand, we have implemented a variable step. Essentially, we have calculated the acceptance rate each 100 iterations of the loop. If it was lower than the 50% the step was multiplied by the factor 1.1. If the contrary occurs, the factor was 0.9. However, we realize that for the clusters up to 50 atoms, the improvement was not significant, so we finally decided to fix s to 0.3.

The local minimisation search routine used in the simulation is a Quasi-Newton method called L-BFGS, since according to the reference [2], it is, at present, the fastest method that can be applied to a large systems. It is a limited-memory quasi-Newton code for bound-constrained optimization, based on the approximation of the Broyden–Fletcher–Goldfarb–Shanno algorithm. The routine mentioned works better if the first derivative of the potential is known analytically. Otherwise, the routine calculates a numerical derivative which increases the computational time required. In the appendix A, the derivatives for both LJ and ILJ potentials are

shown.

4.2 Energies obtained

In chapter 2, the simplest PES was described. Studying the case of the two interacting particles, we can trivially set a lower bound for the energy of the cluster: $-N(N-1)/2$. However, this lower bound can only be reached in the case of N=2, 3 and 4 corresponding to a dimer, equilateral triangle and a regular tetrahedron [3]. Consequently, the other energies will be above the parabola that represents the lower bound.

For the LJ clusters, the curve of the figure 4.1 represents the energy obtained for each of the 50 atoms. The energies and configurations coincide with the ones appeared in The Cambridge Energy Landscape Database [10]. For the atoms $N = 1, ..., 20$ we set a number of 1000 steps. All the minima were found in the first run. For the atoms $N = 21, ..., 50$ we set 5000 steps, with the exception of 10000 steps for the LJ_{38} due to its special geometry which is explained in the next section. In the first run not all the global minima could be found, $N = 27,\ 34,\ 37,\ 38,\ 40,\ 42,\ 43,\ 44,\ 47,\ 48,\ 49,\ 50$ weren't achieved at first. When we run more trajectories, all of them were achieved.

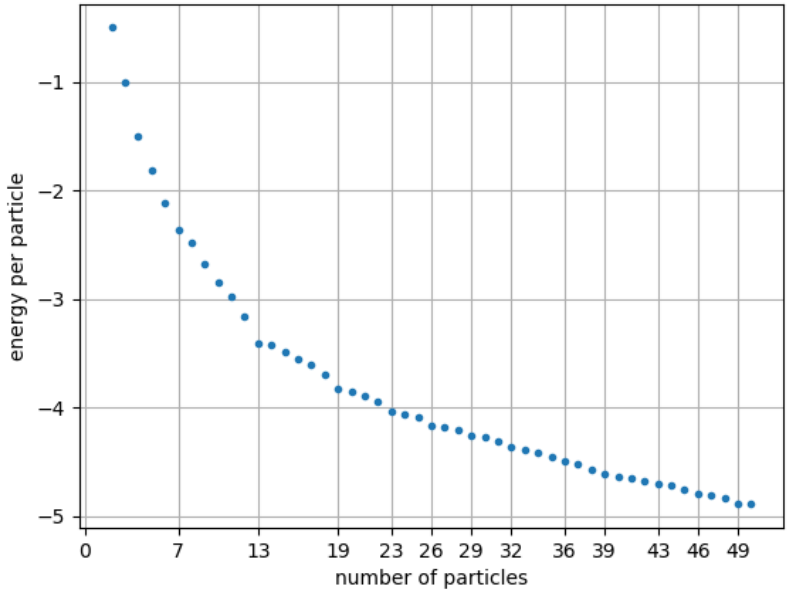

Figure 4.1: Energy per particle for clusters, up to 50 atoms, interacting according to the Lennard-Jones potential.

As we have seen in chapter 2, the ILJ behaviour in the equilibrium range is essentially the same as the LJ. That's why we can see in figure 5.1 that for the first clusters ($N = 2,\ 3,\ 4$) where the distance between atoms is exactly the equilibrium distance, there is no difference in the energies. When N becomes larger the difference of energy per particle between LJ and ILJ increases. This happens due to the fact that the structure becomes more strained.

Although the energies of the clusters are different depending on the potential we

use to describe them, the structure they form is essentially the same.

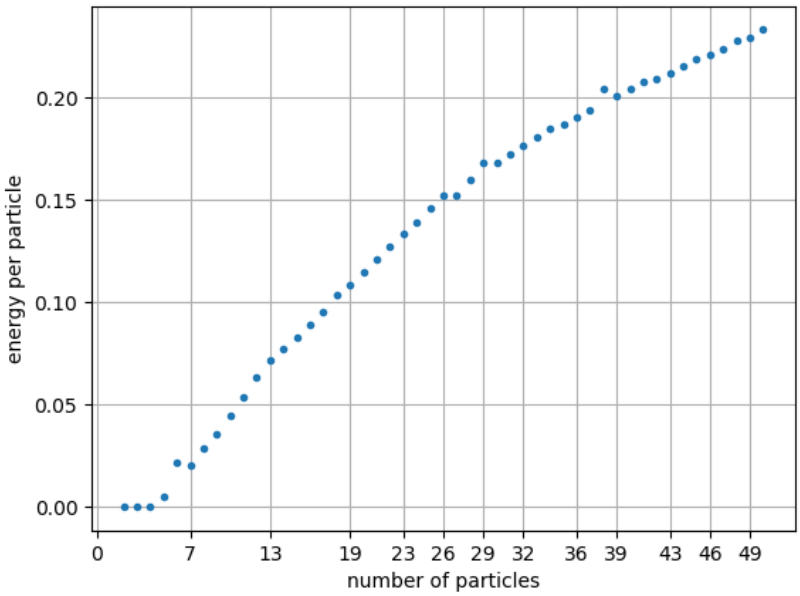

Figure 4.2: Difference of energy per particle between LJ and ILJ potentials, $(ILJ - LJ)/N$.

4.3 Summary in Spanish

En nuestra simulación se han usado unidades que consideran que $\sigma = 1$, $\epsilon = 1$ y $r_m = 2^{1/6}$, a parte de $k_B = 1$.

En la primera parte del capítulo, se explican todos los pasos necesarios que se han implementado en el programa, así como formas de reducir el tiempo computacional. En la segunda parte, se muestran los resultados obtenidos para las energías y las desviaciones en energías de un potencial frente al otro. Ha de tenerse en cuenta que aunque las energías calculadas mediante ambos potenciales difieran, las estructuras que forman las configuraciones de mínima energía son esencialmente las mismas.

Chapter 5

Stability and geometries

This chapter aims to describe the geometries that are usually found in LJ and ILJ clusters. It contains information about the most interesting cases we have treated, as they are: the complete icosahedron in N=13 and the challenging truncated octahedron in N=38. It also contains results of the trajectories we have run and clarifying pictures of the structures obtained.

5.1 Stability

It is well-known that the second-order energy difference is a sensitive physical parameter which gives information about the stability of the cluster [12]. It is denoted as $\Delta_2 E(N)$ and it is defined trough the equation

$$\Delta_2 E(N) = E(N+1) + E(N-1) - 2E(N) \tag{5.1}$$

In the figure 5.1 we have represented the second-order energy difference for both LJ and ILJ. We can realise that some of the peaks of the figure 5.1 correspond to lower points in the figure 4.1. That's because they have more stability than the clusters of the surroundings. It is specially notorious the case of the $N = 13$ and $N = 19$, we talk about these configurations in the next sections.

5.2 Common structures in clusters

The most common packing scheme exhibit by LJ and ILJ clusters are based on icosahedron. The icosahedron is a polyhedron with 20 faces of equilateral triangles, 30 edges and 12 vertices (faces+vertices-edges=2 for a platonic solid). The figure 5.2 shows the cited configuration [2].

Many different clusters of atoms can be described as layers of close-packed atoms stacked on top of each other. Hexagonal-close-packed (hcp) and face-centered-cubic (fcc) patterns are two very common close-packing schemes [2]. The majority of the LJ clusters are based on icosahedral packing via an underlying Mackay icosahedron [2]. In a complete Mackay icosahedron the close packing scheme is fcc, while anti-Mackay icosahedron corresponds to a hcp.

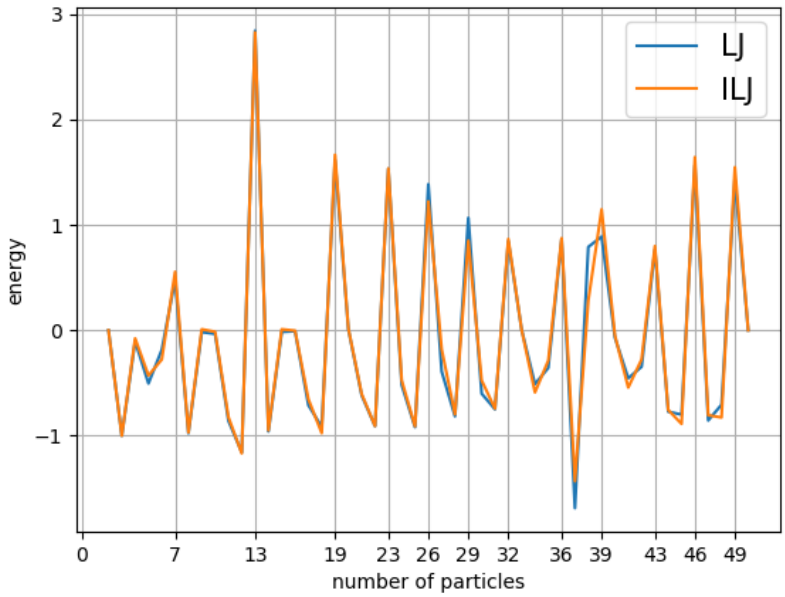

Figure 5.1: Second-order energy difference for both LJ and ILJ

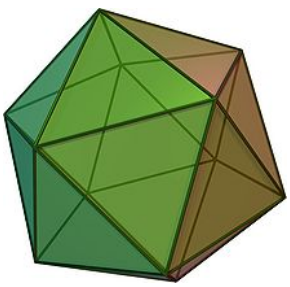

Figure 5.2: Geometry of an icosahedron

The number of atoms that forms a complete Mackay icosahedron is obtained through

$$\frac{1}{3}(10n^3 + 15n^2 + 11n + 3), \qquad n = 1,\ 2,\ 3, \ldots \ , \tag{5.2}$$

which leads to the sequence $N = 13,\ 55,\ 147,\ 309...$ The numbers of this sequence are also known in this context as "magic numbers" because of the notorious stability of their associated configuration.

As the icosahedron has only 12 vertices, the $N = 13$ is due to an atom which is inside the configuration. Due to this atom, the edges are about 5% less than the equilibrium distance [2].

Icosahedra is more strained than other structures due to the deviation of the near-neighbour distance from the equilibrium separation. Increasing the size of the cluster, this effect increases, that's why there will be a point where other structures became more stable. But this is still an area of research [2].

When the number of atoms does not form a complete icosahedral, the structure is usually described as a complete Mackay icosahedron with a layer of some sort.

If the global minimum is not based on an icosahedral structure, as we have said before, it is interesting testing the global optimization methods in that cluster. This happens in $N = 38,\ 75 - 77,\ 98,\ 102 - 104$. The cited cases occurs when there is an specially stable non-icosahedral structure in addition to having an unstable incomplete overlayer [2]. In the figure 5.3 we can see the non icosahedral energy minimum structure mentioned, with the exception of the Leary tetrahedron that occurs in $N = 98$.

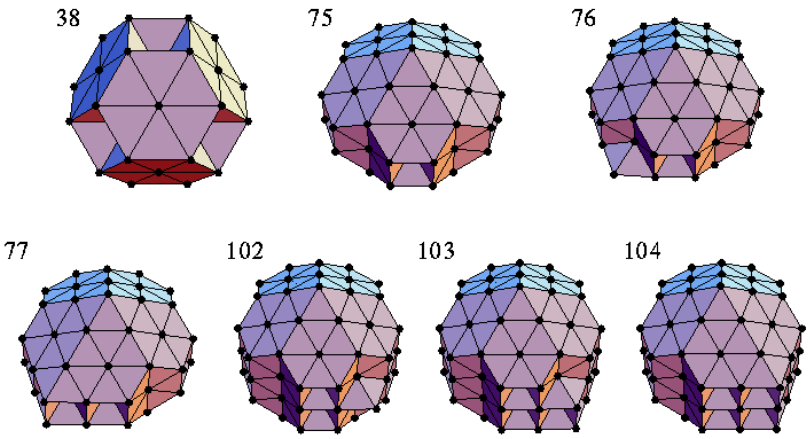

Figure 5.3: Global energy minimum structures based on non-icosahedral packing. LJ_{38}, LJ_{75-77} and $LJ_{102-104}$ corresponding to a truncated octahedron (the first one) and Marks decahedra (all the others). Image extracted from the reference [2]

In the sections below we are going to discuss about the interesting structures

we have obtained (up to 50 atoms): LJ_{13}-ILJ_{13} icosahedron, LJ_{38}-ILJ_{38} truncated octahedra and some more.

5.3 LJ_{13} and ILJ_{13} icosahedra

$N = 13$ cluster has a special stability due to the fact that it forms a complete Mackay icosahedron. It can be shown in the figure 5.4. It doesn't present any difficulty to find the minimum. There is no other structure that compete with the icosahedron. In fact, the next three lowest energy structures corresponds to an icosahedron with one atom removed and placed in another layer. Moreover, there is a relative large energy gap between the Mackay icosahedron and the next lowest energy, the energy gap is: 2.85ϵ [2].

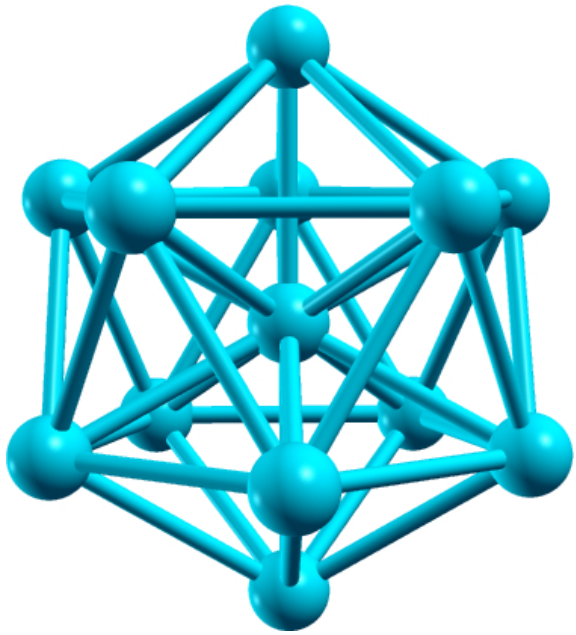

Figure 5.4: Structure of the global energy minimum of the cluster N=13. Image represented by means of the program XCrySDen. [13]

In the figure 4.1, we can see that the energy per particle of N=13 is almost the same as N=14. That is in concordance with the special stability of this cluster.

5.4 LJ_{38} and ILJ_{38} the truncated octahedra

The cluster corresponding to $N = 38$ presents, by far, the most challenging global minimum search we have done. In this case, we have two competing alternative morphologies. On the one hand, they are structures based on icosahedra and on the other hand we have the face-centered cubic truncated octahedron. This last one structure corresponds to the global energy minimum configuration. In figure 5.6 it is shown the structure based on icosahedra, whilst the truncated octahedron is shown in figure 5.5

For the Lennard-Jones potential, we set 10000 steps and we run 10 trajectories. The results are shown in the table 5.1. The three energies obtained are the lowest energies of the corresponding PES [2].

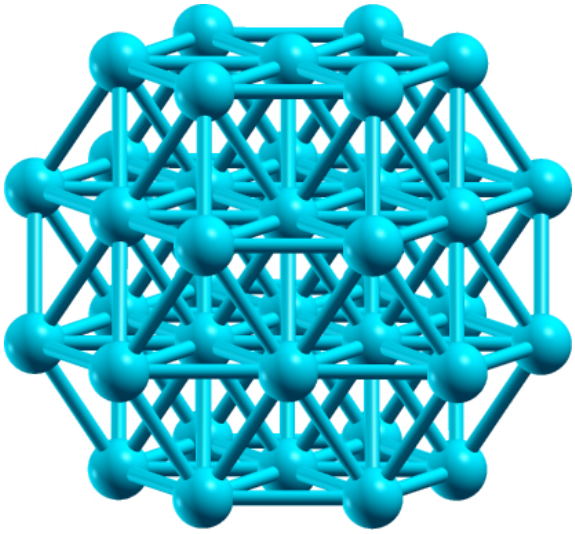

Figure 5.5: Structure based on a trucated octahedron of the cluster N=38 (lowest energy structure). Image represented by means of the program XCrySDen. [13]

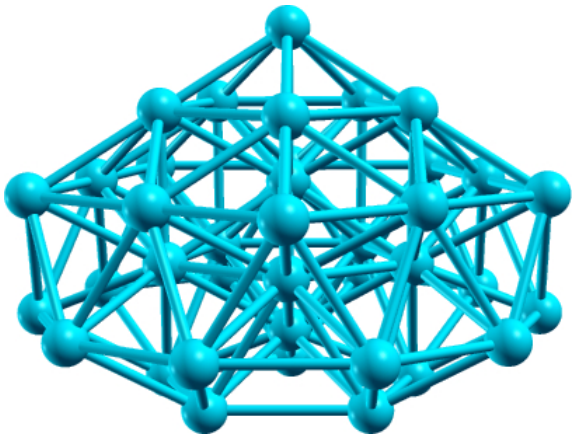

Figure 5.6: Structure based on icosahedron of the cluster N=38 (second lowest energy structure). Image represented by means of the program XCrySDen. [13]

Energy (LJ)	Step	Structure
-173.928426	351, 755, 3058 5415, 5688, 9776	T.O (fcc)
-173.252378	1415, 2660	I.M.I
-173.134317	3580, 3916	I.M.I

Table 5.1: Results obtained for the 10 trajectories performed for LJ_{38}. T.O designs truncated octahedron and I.M.I incomplete Mackay icosahedron.

For the Improved Lennard-Jones, we performed, at first, two trajectories with 10000 iterations. Both of them, result in an incomplete Mackay icosahedron: the second lowest energy of the PES. We decided to set much more iterations, 50000, although it takes a lot of computational time and we run other 4 trajectories. However, all of them got trapped in the second lowest energy. We decided to take a different approach, we set again the number of iterations in 10000 and increase the temperature to 0.9 and the step to 0.4, in order to explore more the PES. After changing the temperature, 8 more trajectories were run, obtaining finally the global minimum in all of them. The results are shown in the table 5.2

Energy (ILJ)	Step	Structure
-166.167427	828, 9554, 9658, 4609, 4626, 5191, 6959, 7720	T.O (fcc)
-165.792799	1627, 7964, 21837, 3536, 239029, 48790	I.M.I

Table 5.2: Results obtained for the 14 trajectories performed for the ILJ_{38} cluster.

5.5 Other interesting cases

The notorious peaks in N=19, 23 and 26 observed in the figure 5.1 correspond to double, triple and quadruple interpenetrating icosahedra. Configurations for N=19 and N=26 can be observed in figures 5.7 y 5.8. In this case, they are formed by anti-Mackay overlayer growth [2].

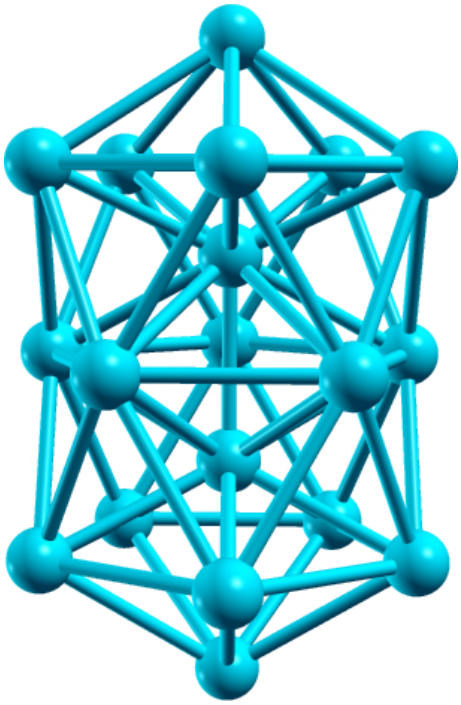

Figure 5.7: Structure of global energy minimum of the cluster N=19. Image represented by means of the program XCrySDen. [13]

Another interesting structure is the corresponding to $N = 45$. Although, its second-order energy difference indicates that it has not remarkable stability, it has a complete anti-Mackay overlayer. This configuration is shown in the figure 5.9.

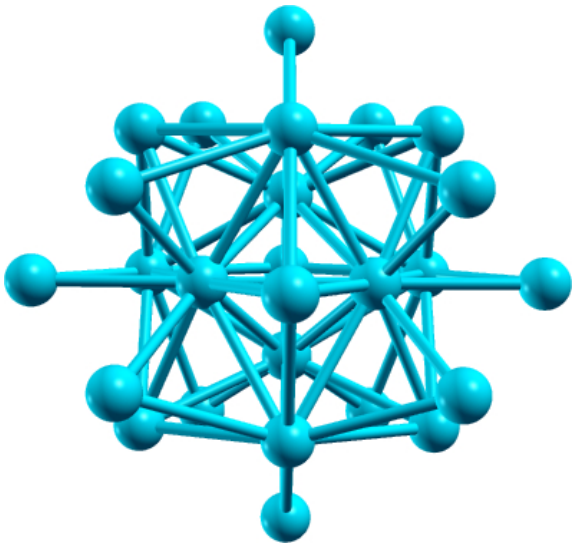

Figure 5.8: Structure of global energy minimum of the cluster N=26. Image represented by means of the program XCrySDen. [13]

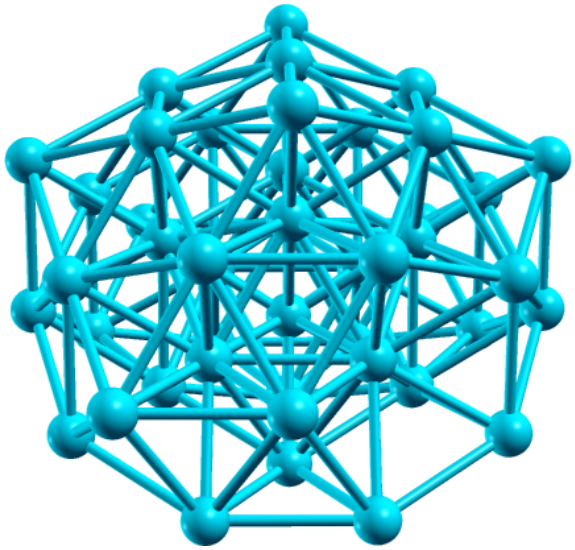

Figure 5.9: Structure of global energy minimum of the cluster N=45. Image represented by means of the program XCrySDen. [13]

5.6 Summary in Spanish

En este capítulo se describe la estabilidad de los agregados de átomos mediante las diferencias de segundo orden de la energía. Los picos de la gráfica se asocian a los agregados especialmente estables. A continuación, se discute sobre las estructuras geométricas más comunes para los agreagados de átomos, centrándonos especialmente en el icosaedro de Mackay, el cual constituye la principal geometría para los agregados de LJ e ILJ. Finalmente, se incluyen secciones que explican los casos más relevantes tratados. El icosaedro de Mackay completo en N=13 debido a su gran estabilidad y el octaedro truncado en N=38 debido a la dificultad para encontrarlo. También se destacan otros casos debido a su especial forma geométrica.

Chapter 6

Conclusions

The basin-hopping method is a powerful technique for finding global minimum structure in clusters. We have been able to implement it and obtain, successfully, all the energies minima and its corresponding structures up to $N = 50$ for both LJ and ILJ potentials.

However, in the case of $N = 38$ for the ILJ, we have to performed several trajectories and we couldn't find the global minimum until we change the temperature and the step. It's likely we would have some troubles for next complicated configurations as $N = 75$. In order to overcome this problem, we could implement some improvements to the code. We can implement a variable temperature similarly the way we implement a variable step in chapter 4, and compare with the results we have obtained. As an example we have included a flowchart of a more elaborated version of the basin-hopping that may achieve a better performance [9]. The method considers as variables: the step, the temperature and a new input parameter denoted as ν. ν is a parameter which compared the highest potential, V_h, and the lowest potential, V_l over the particles of the configuration. If $V_h > \nu V_l$ the perturbation is the same as we have implemented, otherwise the atom which has V_h is perturbed in other different way.

With the explanation provided in the chapter 3, the simulated annealing could be easily programmed. However, as we have said previously, the method itself works correctly for clusters containing a few atoms. On the other hand, programming the genetic algorithm could be of great interest due to its promising state of art, and the possibility of comparing it with the basin-hopping, even for larger clusters.

There also exist the possibility of combining methods. That is exactly what was studied in the paper whose reference is [14]. They combined the simulated annealing method and the genetic algorithm in order to create an hybrid method, and analyse its capability of finding the global minimum structure of silicon clusters containing six and ten atoms. The resulting hybrid approach outperformed the SA and GA. In addition, it is said, that the method is, in principle, extensible for any other molecular systems.

To sum up, the global optimization is a relevant and interesting area, which is in growing development. It has many applications and it enables us to solve problems with many degrees of freedom. Lennard-Jones and Improved Lennard-Jones clusters, are an excellent testbed for these methods, due to the simplicity of the analytical form of the potential and to the complex PES that presents some of the clusters, as

it is LJ_{38} and ILJ_{38}.

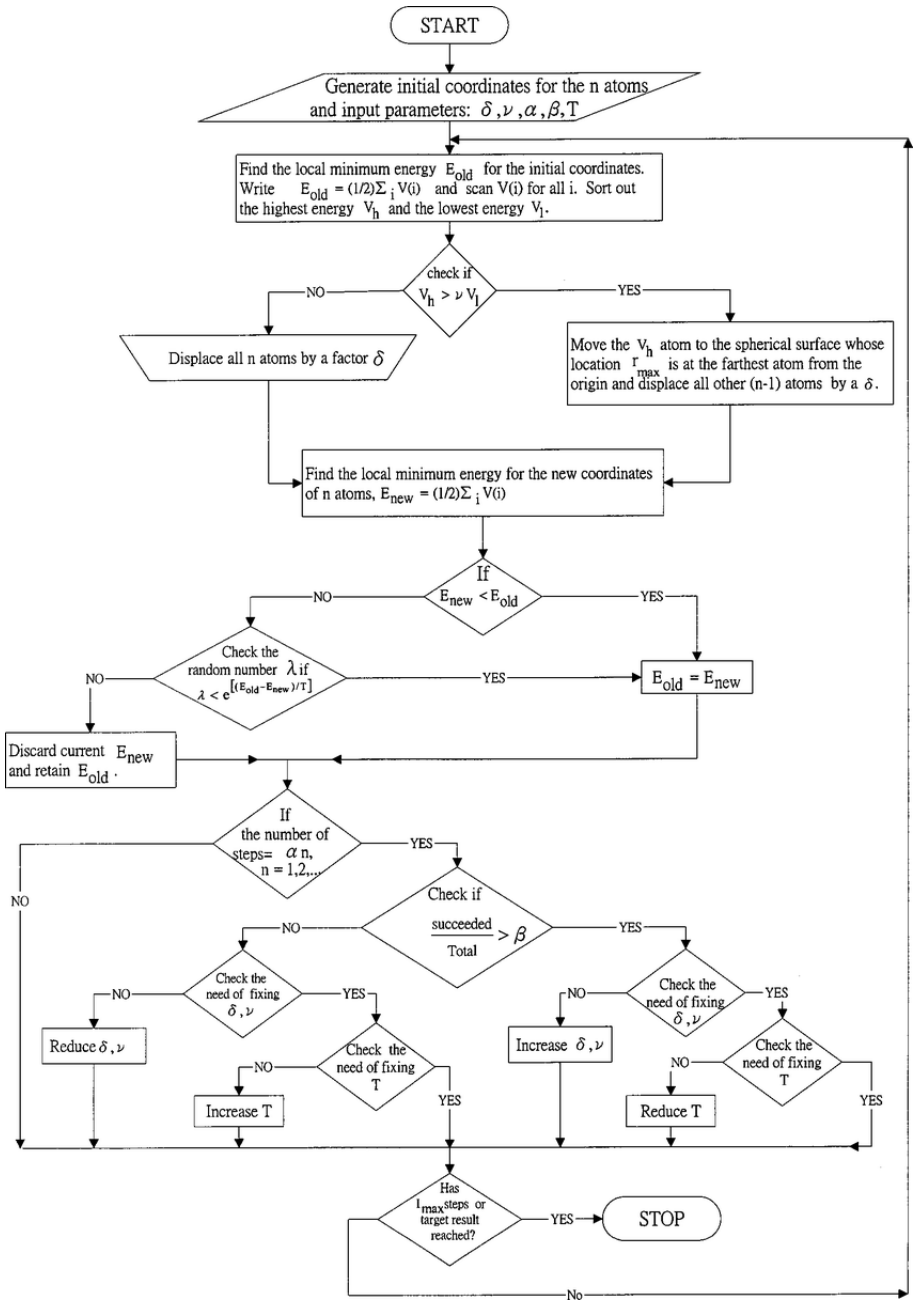

Figure 6.1: Flowchart of an improved basin-hopping algorithm. It is extracted from reference [9]

6.1 Summary in Spanish

El método de optimización de salto de pozos (BH) es una herramienta potente a la hora de encontrar la mínima energía en agregados de átomos. En este proyecto, hemos conseguido encontrar las estructuras de mínima energía para agregados que contienen hasta 50 átomos para el potencial LJ y el ILJ.

Sin embargo, como se vio en el caso N=38 para el potencial ILJ, a la temperatura que se tenía era más dificil encontrar el mínimo global. Es posible que nos encontremos con problemas similares en otras estructuras no basadas en geometría

iscosaédrica. Por consiguiente, sería interesante realizar una mejora al algoritmo de forma que la temperatura varíe según como esté yendo la optimización.

Por otro lado, con la información provista en el trabajo, sería sencillo implementar el algoritmo de enfriamiento simulado. Sin embargo, puede que no sea de gran interés, ya que solo nos permitiría estudiar agregados de pocos átomos. Por el contrario, la implementación del algoritmo genético podría ser de gran interés y permitirnos comparar los resultados con el basin-hopping incluso para sistemas que contengan más átomos.

También existe la posibilidad de combinar métodos para formar un nuevo método híbrido que sea más efectivo que sus predecesores. Este es el caso estudiado en el artículo de la referencia [14], donde se combinó el algoritmo de enfriamiento simulado y el algoritmo genético para la optimización de moléculas de silicio que contenían seis y diez átomos. Este método, en principio es extensible a cualquier otro sistema molecular.

A modo de resumen, la optimización global es un campo relevante que se encuentra en creciente desarrollo. Tiene muchas aplicaciones y permite resolver problemas que tienen muchos grados de libertad. Encontrar el mínimo global de los agregados de átomos que interaccionan según un potencial de LJ o ILJ, es un problema fantástico para comprobar la utilidad de estos métodos, debido a la simplicidad de la forma del potencial y a la complejidad de las PES de los agregados.

Appendix A

Derivatives of the Lennard-Jones and Improved Lennard-Jones potentials

The derivative of the Lennard-Jones potential with respect to the distance between particles is

$$\frac{dV_{LJ}}{dr} = \frac{4\epsilon}{\sigma}\left[6\left(\frac{\sigma}{r}\right)^{7} - 12\left(\frac{\sigma}{r}\right)^{13}\right] \tag{A.1}$$

Meanwhile the derivative for the improved Lennard-Jones

$$\begin{aligned}\frac{dV_{LJ}}{dr} = \frac{\epsilon m}{(n(r)-m)r_m}\Bigg[&n(r)\left(\frac{r_m}{r}\right)^{m+1} - n(r)\left(\frac{r_m}{r}\right)^{n(r)+1} \\ &+8\left(\ln\left(\frac{r_m}{r}\right) - \frac{1}{n(r)-m}\right)\left(\frac{r_m}{r}\right)^{n(r)-1} + \frac{8}{n(r)-m}\left(\frac{r_m}{r}\right)^{m-1}\Bigg]\end{aligned} \tag{A.2}$$

In the figure A.1, the derivatives for both LJ and ILJ are shown.

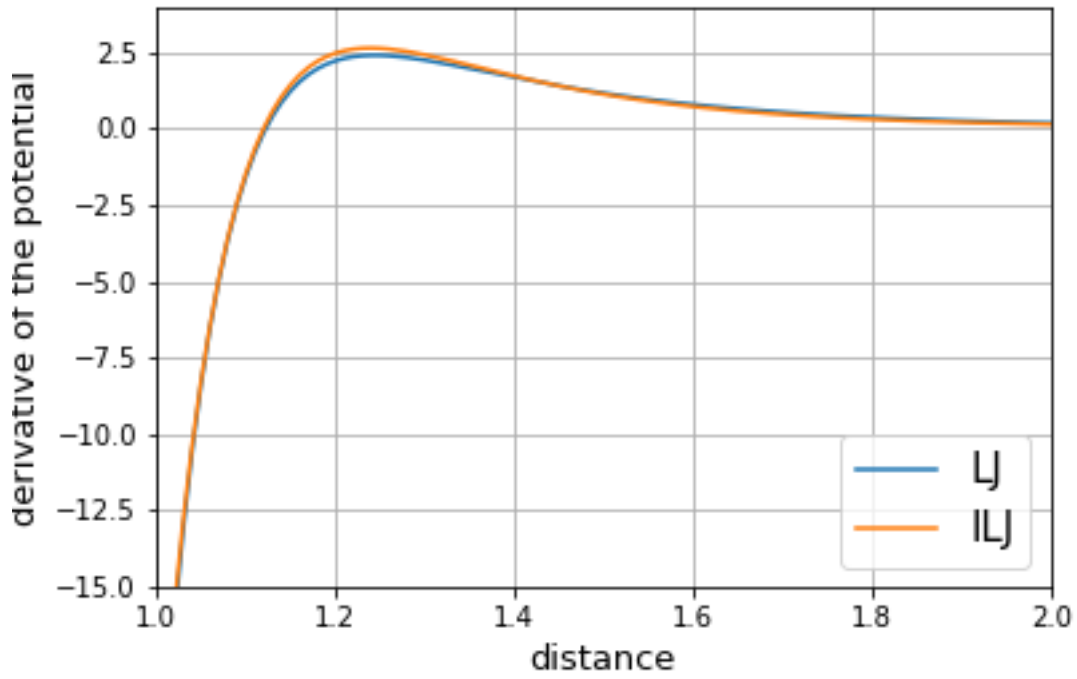

Figure A.1: Derivatives for both LJ and ILJ potentials

Bibliography

[1] D. J. Wales and H. A. Scheraga, "Global optimization of clusters, crystals, and biomolecules," *Science*, vol. **285**, p. 1368, (1999).

[2] D. J. Wales, *Energy Landscapes*. Cambridge University Press, 2003.

[3] L. Wille, "Simulated annealing and the topology of the potential energy surface of lennard-jones clusters," *Computational Materials Science*, vol. **17**, p. 551, (2000).

[4] F. Pirani and collaborators, "Beyond the lennard-jones model: a simple and accurate potential function probed by high resolution scattering data useful for molecular dynamics simulations," *Physical Chemistry Chemical Physics*, vol. **10**, p. 5477, (2008).

[5] R. L. Johnston, "Evolving better nanoparticles: Genetic algorithms for optimising cluster geometries," *Dalton Transactions*, vol. **22**, p. 4193, (2003).

[6] D. J. Wales and J. P. K. Doye, "Global optimization by basin-hopping and the lowest energy structures of lennard-jones clusters containing up to 110 atoms," *The Journal of Physical Chemistry A*, vol. **101**, p. 5111, (1997).

[7] R. Womersley, "Local properties of algorithms for minimizing nonsmooth composite functions," *Mathematical programming*, vol. **32**, 1985.

[8] A. S. Robert Zwanzig and B. Bagchi, "Levinthal's paradox," *Proc Natl Acad Sci U S A.*, vol. **1**, p. 20, (1992).

[9] A. S. K. Lai and collaborators, "Structures of metallic clusters: mono-and polyvalent metals," 2002.

[10] D. J. Wales and collaborators, "The cambridge energy landscape database,"

[11] J. Hernández-Rojas. Private communication.

[12] P. G.-A. Leyva, E. M. Sosa-Hernández, J. M. Montejano-Carrizales, and F. Aguilera-Granja, "Stable geometries and magnetic properties of neutral sn x+ 1 and fesn x (x$\leq$ 8) clusters," *The European Physical Journal D*, vol. **69**, p. 51, (2015).

[13] A. Kokalj, "Computer graphics and graphical user interfaces as tools in simulations of matter at the atomic scale," *Computational Materials Science*, vol. **28**, p. 155, (2003).

[14] C. Zacharias, M. Lemes, and A. D. Pino, "Combining genetic algorithm and simulated annealing: a molecular geometry optimization study," *Journal of Molecular Structure: THEOCHEM*, vol. **430**, p. 29, (1998).